On the Effects of the Tunnel Wall Interference and the Wall Boundary Layer in the Airfoil Cascade Test

By

Gorō KAMIMOTO

Department of Mechanical Engineering

(Received August 31, 1957)

Abstracts

This paper deals with the theoretical calculation of the wind tunnel interference in the cascade tests under the assumption of two-dimensional potential flow and then with the interference of the wall boundary layer upon the turning angle of flow in the cascade. Part I contains the theory of the wind tunnel wall interference upon the turning angle and Part II, the theory of the tunnel wall interference upon the airfoil characteristics in the cascade composed of airfoils having arbitrary shapes. A numerical example is shown in the case of cascade composed of N.A.C.A. 6409 and compared with some experimental results. Finally, Part III contains the methods of calculating the wall boundary layer effects upon the turning angle.

1. Introduction

In an ordinary cascade test, as shown in Fig. 1, the finite numbers of airfoils are arranged at the exit of the channel bounded by the two parallel walls and the aerodynamic characteristics, such as lift, drag and pressure distribution and so on, are usally measured at the airfoil centering among the others. And, also, the turning angle θ between the inlet and exit flow in the cascade is often measured[1]. The author had previously discussed the tunnel wall interference[2] in the various types of cascade tests

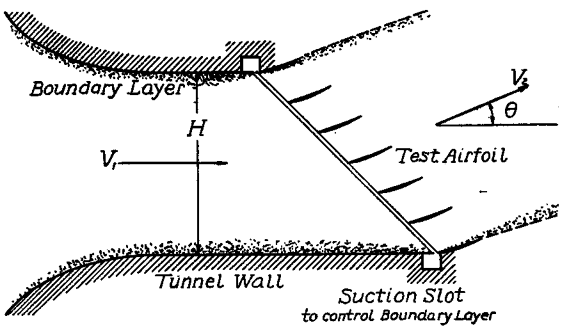

Fig. 1

with the finite numbers of airfoils and calculated theoretically the cascade interference factor of lift by means of the conformal representation.

In this paper, at first the tunnel wall interference upon the turning angle is calculated by means of the other conformal mapping under the various cascade conditions. Next, the thin arirfoil theory of Glauert is applied to the cascade composed of airfoils with arbitrary shape and the aerodynamic characteristics, such as pressure distribution and lift, are theoretically calculated on each airfoil under the induced velocities and their gradients due to the above wall interference. Lastly, the influence of the wall boundary layer upon the turning angle is calculated by the above mapping, assuming an imaginary source distribution, which is equivalent to the displacement thickness distribution of the wall boundary layer. The results obtained made clearer the physical meanings of the suction slots, which are bored on the inlet walls of the cascade used in the recent tests[3].

Part I
Wind Tunnel Wall Interference upon Turning Angle

2. Conformal Mapping

Suppose a figure composed of infinite numbers of parallel half-straight lines with the distance H and the stagger angle β_1 in the z-plane, as shown in Fig. 2. Taking

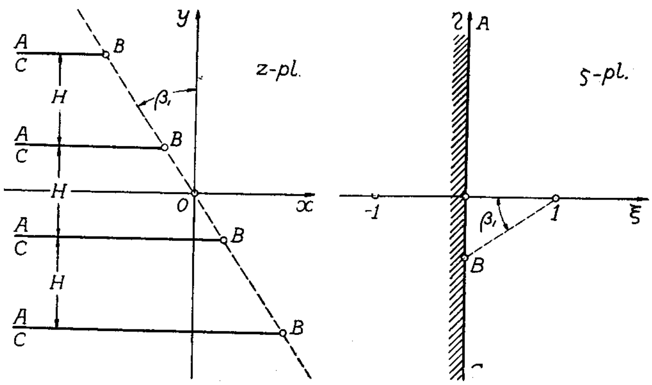

Fig. 2

the origin of the z-plane at such a position as shown in Fig. 2., the exterior domain of the contours in the z-plane can be conformally transformed into the right side domain in the ζ-plane by the following function;

$$
\begin{aligned}
z = & -\frac{H}{2\pi}\{(1+i\tan\beta_1)\log(\zeta-1)+(1-i\tan\beta_1)\log(\zeta+1)\} \\
& -\frac{H}{\pi}(\log\cos\beta_1+\beta_1\tan\beta_1)
\end{aligned}
\tag{1}
$$

The straight lines, i. e. tunnel walls ABC, correspond to the η-axis in the ζ-plane and the points $z=\pm\infty$ respectively to $\zeta=\pm 1$ and $\zeta=\infty$. From the eq. (1)

$$\left.\begin{aligned} \frac{dz}{d\zeta} &= -\frac{H}{\pi}\frac{\zeta+i\tan\beta_1}{\zeta^2-1} \\ \left|\frac{dz}{d\zeta}\right|_{\zeta=i\eta} &= \frac{dx}{d\eta} = \frac{H}{\pi}\frac{\eta+\tan\beta_1}{\eta^2+1} \end{aligned}\right\} \tag{2}$$

and the edge points B of the tunnel walls correspond to the following position on the η-axis;

$$\eta = -\tan\beta_1\,. \tag{3}$$

The wall distance H is given as follows in the case of an arrangement of cascade airfoils as shown in Fig. 1 by denoting the chord length of airfoil as c and the pitch d;

$$H = Zd\cos\beta_1 = 2(N+1)\,d\cdot\cos\beta_1$$

where Z is the number of airfoils, and $Z=2(N+1)$.

Letting the corresponding points on the ζ-plane to the 1/4-chord points from the leading edge on each airfoil be $\kappa e^{i\gamma}$ $(-\kappa e^{-i\gamma})$, then κ and γ can be determined by the following relations;

$$\begin{aligned} &\log\sqrt{1-2\kappa\cos\gamma+\kappa^2}+\log\sqrt{1+2\kappa\cos\gamma+\kappa^2} \\ &\quad -\tan\beta_1\left\{\tan^{-1}\frac{\kappa\sin\gamma}{\kappa\cos\gamma-1}-\tan^{-1}\frac{\kappa\sin\gamma}{\kappa\cos\gamma+1}\right\} \\ &= -\frac{\pi}{N+1}\left(\frac{\sec^2\beta_1}{\lambda}+n\tan\beta_1\right)-2(\log\cos\beta_1+\beta_1\tan\beta_1)\,, \\ &\tan\beta_1\{\log\sqrt{1-2\kappa\cos\gamma+\kappa^2}-\log\sqrt{1+2\kappa\cos\gamma+\kappa^2}\} \\ &\quad +\tan^{-1}\frac{\kappa\sin\gamma}{\kappa\cos\gamma-1}+\tan^{-1}\frac{\kappa\sin\gamma}{\kappa\cos\gamma+1} = \frac{n\pi}{N+1} \end{aligned} \tag{4}$$

where λ is the pitch-chord ratio, and n the airfoil number, as shown in Fig. 3, then $n=0,\ \pm1,\ \pm2,\ \pm3, \cdots, \pm N$ and $N+1$.

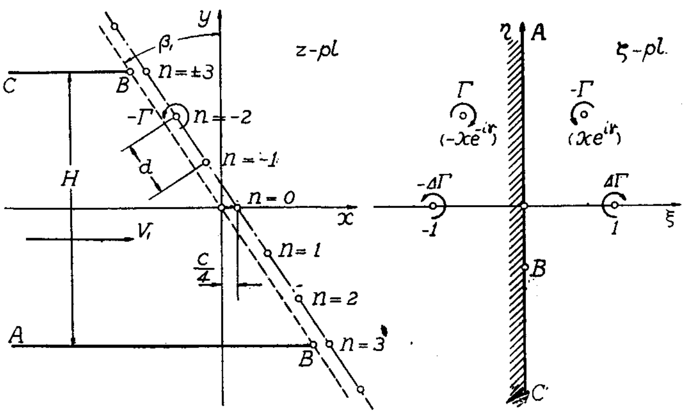

Fig. 3

3. Complex Potential Function

The complex potential function on the ζ-plane, which corresponds to the uniform flow among the parallel walls, can be expressed as follows according to the above mapping function;

$$F_0(\zeta) = -\frac{V_1 H}{2\pi}\log(\zeta^2-1)+\frac{i\Gamma_0}{2\pi}\log\frac{\zeta+1}{\zeta-1} \tag{5}$$

where V_1 is the uniform velocity in the wind tunnel and Γ_0 an unknown magnitude of circulation, the one of which can be determined by the condition that the flow should flow out smoothly from the edge points B ($\zeta=-i\tan\beta_1$) as follows;

$$\Gamma_0 = V_1 H\tan\beta_1 \tag{6}$$

Further, the flow due to one airfoil with the circulation Γ among the cascade airfoils, arranged at the wind tunnel, can be expressed by the following function $F_1(\zeta)$;

$$F_1(\zeta) = -\frac{i\Gamma}{2\pi}\log\frac{\zeta-\kappa e^{i\gamma}}{\zeta+\kappa \bar{e}^{i\gamma}}-\frac{i\Delta\Gamma}{2\pi}\log\frac{\zeta+1}{\zeta-1} \tag{7}$$

where $\Delta\Gamma$ is an unknown quantity of circulation put into the points $\zeta=\pm1$ on the ζ-plane. The magnitude of $\Delta\Gamma$ can be also determined by the above-mentioned condition;

$$\left|\frac{dF_1}{d\zeta}\right|_{\zeta=-i\tan\beta_1} = 0 \tag{8}$$

Then, $\Delta\Gamma$ becomes as

$$\frac{\Delta\Gamma}{\Gamma} = \frac{\kappa\cos\gamma\cdot\sec^2\beta_1}{\tan^2\beta_1+2\kappa\sin\gamma\cdot\tan\beta_1+\kappa^2}. \tag{9}$$

Thus, the induced velocities at the points $z=\pm\infty$ on the z-plane is obatined as follows;

$$\left.\begin{aligned} \left|\frac{dF_1}{dz}\right|_{z=-\infty} &= \left|\frac{dF_1}{d\zeta}\frac{d\zeta}{dz}\right|_{\zeta=\infty} = 0 \\ \left|\frac{dF_1}{dz}\right|_{z=\infty} &= \left|\frac{dF_1}{d\zeta}\frac{d\zeta}{dz}\right|_{\zeta=1} = -\frac{\Delta\Gamma}{H}\sin\beta_1\cdot\cos\beta_1-i\frac{\Delta\Gamma}{H}\cos^2\beta_1. \end{aligned}\right\} \tag{10}$$

Then, the velocity at the upstream tunnel is the uniform velocity V_1, and the velocity and direction of the downstream are changed by the circulation Γ. Denote the induced velocity components at the downstream as Δu_∞ and Δv_∞ respectively to the x- and y-axis, then

$$\frac{\Delta u_\infty}{V_1} = -\frac{\Delta\Gamma}{V_1 H}\sin\beta_1\cdot\cos\beta_1$$

and

$$\frac{\Delta v_\infty}{V_1} = \frac{\Delta\Gamma}{V_1 H}\cos^2\beta_1. \tag{11}$$

Therefore, assuming that each airfoil has the same magnitude Γ of circulation, the induced velocity components u_∞ and v_∞ at the cascade composed of the numbers $Z=2(N+1)$ of airfoils, are expressed as follows;

$$\left.\begin{aligned}\frac{u_\infty}{V_1} &= \sum_{n=-N}^{N+1}\frac{\Delta u_\infty}{V_1} = -\frac{\Gamma}{V_1H}\tan\beta_1\sum_{n=-N}^{N+1}\frac{\kappa\cos\gamma}{\kappa^2+2\kappa\sin\gamma\cdot\tan\beta_1+\tan^2\beta_1}\\ \frac{v_\infty}{V_1} &= \sum_{n=-N}^{N+1}\frac{\Delta v_\infty}{V_1} = \frac{\Gamma}{V_1H}\sum_{n=-N}^{N+1}\frac{\kappa\cos\gamma}{\kappa^2+2\kappa\sin\gamma\cdot\tan\beta_1+\tan^2\beta_1}\,.\end{aligned}\right\}\tag{12}$$

Then, the exit velocity V_2 and the turning angle θ at the cascade test become as

$$\left.\begin{aligned}V_2 &= V_1\sqrt{\left(1+\frac{u_\infty}{V_1}\right)^2+\left(\frac{v_\infty}{V_1}\right)^2}\\ \text{and}\qquad \tan\theta &= \left(\frac{v_\infty}{V_1}\right)\Big/\left[1+\left(\frac{u_\infty}{V_1}\right)\right]\end{aligned}\right\}\tag{13}$$

Also denoting the velocity of flow along the tunnel wall as w, the result of some calculations gives the velocity w as follows;

$$w = V_1\left\{1+\left(\frac{\Gamma}{V_1H}\right)\sum_{n=-N}^{N+1}\frac{\kappa\cos\gamma(\eta^2+1)-\left(\frac{\Delta\Gamma}{\Gamma}\right)(\eta^2-2\kappa\sin\gamma\cdot\eta+\kappa^2)}{(\eta+\tan\beta_1)(\eta^2-2\kappa\sin\gamma\cdot\eta+\kappa^2)}\right\}\tag{14}$$

and the velocity w at the edge B is given as

$$w_B = V_1\left\{1+2\left(\frac{\Gamma}{V_1H}\right)\sum_{n=-N}^{N+1}\frac{\kappa\cos\gamma\{(1-\kappa^2)\tan^2\beta_1+\kappa\sin\gamma(1-\tan^2\beta_1)\}}{\tan\beta_1(\tan^2\beta_1+2\kappa\sin\gamma\cdot\tan\beta_1+\kappa^2)}\right\}.\tag{15}$$

4. Tunel Wall Interference of Turning Angle

Comparing the above obtained turning angle θ with θ_∞, the one in the cascade composed of infinite numbers of airfoils, the tunnel wall interference upon the turning angle can be calculated. In the latter cascade the turning angle θ_∞ can be given easily by the so-called velocity diagram;

$$\sin\theta_\infty = \frac{\left(\frac{\Gamma}{V_1C}\right)\cos\beta_1}{\sqrt{\lambda^2-2\lambda\left(\frac{\Gamma}{V_1C}\right)\sin\beta_1+\left(\frac{\Gamma}{V_1C}\right)^2}},\tag{16}$$

where $\Gamma/V_1C=C_{L_1}/2$ and C_{L_1} is the lift coefficient referved to the inlet velocity V_1.

As numerical examples, the turning angle θ and θ_∞ are plotted, as shown in Fig. 4, to the angle β_1 under the following conditions; pitch-chord ratio $\lambda=d/c=1$, $\Gamma/V_1C=C_{L_1}/2=0.1$, 0.2, 0.3, 0.4, 0.5, and $Z=2(N+1)=4$, 6, 8. In the figure the negative valus of β_1 show the cascade for the accelerated flow, such as the turbine blade cascade, and the positive values of β_1 show the one for the retarded flow, such as the pump blade cascade. From the calculated results, it is seen that the turning angle θ of the cascade test is larger than θ_∞ of the ideal cascade composed of infinite numbers of airfoils owing to the tunnel wall interference and then it approaches more to θ_∞ as the number of Z becomes greater.

Similarly, at the other cascade having different arrangements, the turning angles θ are calculated under the same conditions and shown in Fig. 5 and 6.

In the above-mentioned cases, the circulation Γ around each airfoil in the cascade is assumed to be of equal magnitude to each other. In the case of a circulation with different magnitudes, the turning angle θ can be calculated by the following relations;

$$\left.\begin{aligned} \frac{u_\infty}{V_1} &= -\tan\beta_1 \sum_{n=-N}^{N+1}\left(\frac{\Gamma}{V_1 H}\right)\frac{\kappa\cos\gamma}{\kappa^2+2\kappa\sin\gamma\cdot\tan\beta_1+\tan^2\beta_1}\,, \\ \frac{v_\infty}{V_1} &= \sum_{n=-N}^{N+1}\left(\frac{\Gamma}{V_1 H}\right)\frac{\kappa\cos\gamma}{\kappa^2+2\kappa\sin\gamma\cdot\tan\beta_1+\tan^2\beta_1}\,. \end{aligned}\right\} \tag{17}$$

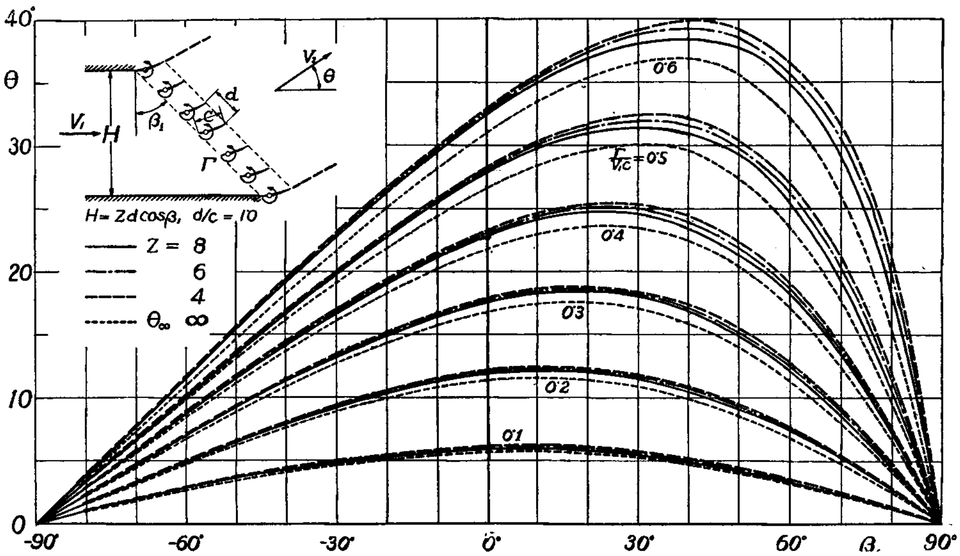

Fig. 4

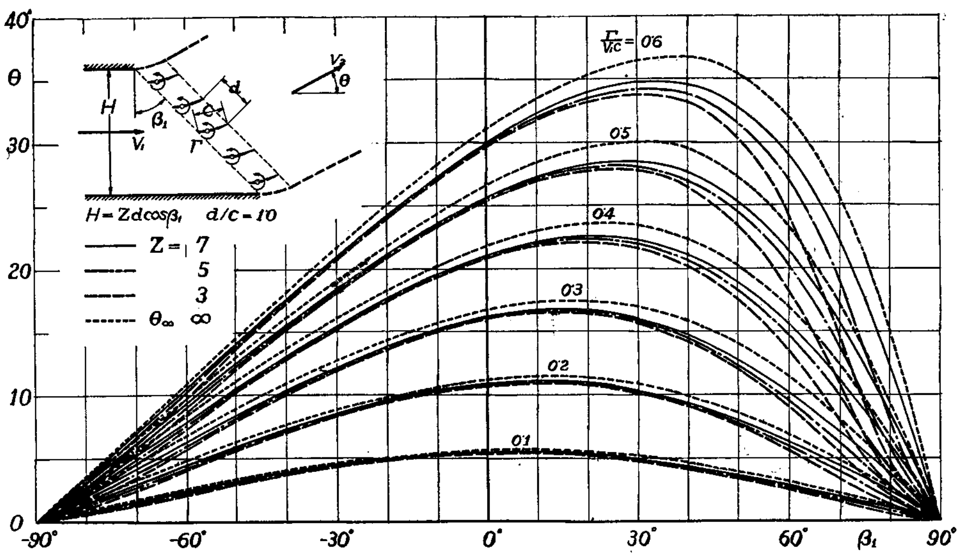

Fig. 5

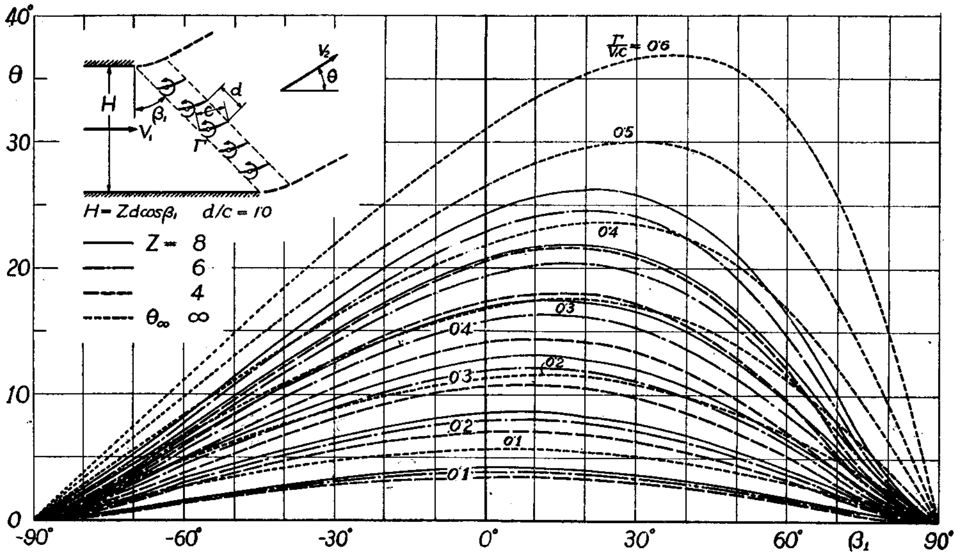

Fig. 6

Part II

Tunnel Wall Interference upon Airfoil Characteristics in Cascade

5. Theory of Cascade[4] by Glauert's Thin Airfoil Theory

In Part I, the theory of cascade is dealt under the assumption that each airfoil can be expressed by the single vortex with the circulation Γ, which is put on the 1/4-chord point from the leading edge, for any shape of airfoil. Assume here that each airfoil has a circulation distribution along the chord of airfoil corresponding to the shape and the cascade conditions.

The profile of airfoil in cascade can be expressed by a camber line y_c and a half thickness distribution y_d with a parameter θ as follows;

$$y_c = \sum_{n=0}^{\infty} a_n \cos n\theta\,, \qquad y_d = \sum_{n=1}^{\infty} b_n \sin n\theta \tag{18}$$

where a_n and b_n are the coefficients determined by a given arifoil shape, ond n is a positive integer. Then, denoting the relation;

$$\frac{dy_c}{dx} = -\sum_{n=1}^{\infty} c_n \cos n\theta \tag{19}$$

where c_n is the coefficients determined by the camber line of a given airfoil, the coefficients c_n can be determined as follows;

$$c_0 = -\sum_{0}^{\infty} (2n+1)\, a_{2n+1}$$

$$
\begin{aligned}
c_1 &= -2\sum_1^\infty 2na_{2n} \\
c_2 &= -2\sum_1^\infty (2n+1)\,a_{2n+1} \\
c_2 &= -2\sum_2^\infty 2na_{2n} \\
c_4 &= -2\sum_2^\infty (2n+1)\,a_{2n+1} \\
&\cdots\cdots\cdots\cdots\cdots\cdots .
\end{aligned}
\tag{20}
$$

Now, denote the velocities along the upper and lower surfaces of airfoil respectively as w_u and w_l, the mean velocity of the inlet and outlet velocities of the cascade as V, then $\gamma = w_u - w_l$ gives the distribution of circulation and $w_d = \frac{1}{2}\cdot(w_u + w_l) - V$ gives the velocity increment due to the thickness, as well known in the Thin Airfoil Theory.

Take the x-axis in the direction of the chord, the abscissa of the trailing edge at $x=1$, and that of the leading edge at $x=-1$, and substitute $x=\cos\theta$, and develope γ and w_d into the following series;

$$
\left.
\begin{aligned}
\frac{\gamma}{2V} &= A_0 \tan\frac{\theta}{2} + \sum_{n=1}^\infty A_n \sin n\theta \\
\text{and}\qquad \frac{w_d}{V}\sin\theta &= \sum_{n=1}^\infty B_n \sin n\theta ,
\end{aligned}
\right\}
\tag{21}
$$

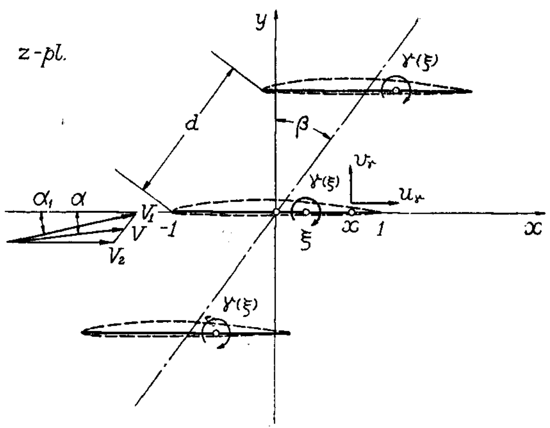

Fig. 7

where A_n and B_n are the unknown coefficients determined by the boundary conditions.

Now, suppose the circulation distribution $\gamma(\xi)$ along the chord and the source-sink distribution $q(\xi)$ along it, which is determined by the half-thickness distribution, where ξ expresses the position of the point on the chord, as shown in Fig. 7. Then, the induced velocity components at the point $\xi = x$, due to the above-mentioned distribution, are given respectively as follows;

$$
\left.
\begin{aligned}
u_\gamma - iv_\gamma &= \frac{ie^{i\beta}}{2d}\int_{-1}^{1} \gamma(\xi)\coth\left[\frac{\pi}{d}e^{i\beta}(x-\xi)\right]d\xi \\
u_q - iv_q &= \frac{e^{i\beta}}{2d}\int_{-1}^{1} q(\xi)\coth\left[\frac{\pi}{d}e^{i\beta}(x-\xi)\right]d\xi
\end{aligned}
\right\}
\tag{22}
$$

where β is the stagger angle of the cascade which has a relation to the angle β_1 and inlet incidence angle α_1 of $\beta_1=\beta+\alpha_1$. Insert the upper eq. of eq. (21) into the upper eq. of eq. (22) and develope the term coth, then

$$\left.\begin{aligned}\frac{u_\gamma}{V} &= -\frac{\pi^2}{24\lambda^2}\sin 2\beta\cdot\left(A_0-\frac{A_2}{2}\right)-\frac{\pi^2}{12\lambda^2}\sin 2\beta\cdot\left(A_0+\frac{A_1}{2}\right)\cos\theta\,,\\ \frac{v_\gamma}{V} &= -A_0-\sum_{n=1}^{\infty}A_n\cos n\theta-\frac{\pi^2}{24\lambda^2}\cos 2\beta\cdot\left(A_0-\frac{A_2}{2}\right)-\frac{\pi^2}{12\lambda^2}\cos 2\beta\cdot\left(A_0+\frac{A_1}{2}\right)\cos\theta\,,\end{aligned}\right\}\quad(23)$$

where $\lambda=d/2$ is the pitch-chord ratio. Determine the source distribution $q(\xi)$ by means of the above induced velocity gradients along the chord, then the velocity components u_q and v_q can be given from the lower eq. of eq. (22) as follows;

$$\left.\begin{aligned}\frac{u_q}{V} &= \frac{\pi^2}{24\lambda^2}\cos 2\beta\cdot b_1+\left\{1-\frac{\pi^2}{24\lambda^2}\sin 2\beta\cdot\left(A_0-\frac{A_2}{2}\right)\right\}\sum_{n=1}^{\infty}nb_n\frac{\sin n\theta}{\sin\theta}\\ &\quad-\frac{\pi^2}{24\lambda^2}\sin 2\beta\cdot\left(A_0+\frac{A_1}{2}\right)\sum_{n=1}^{\infty}nb_n\frac{\sin(n+1)\theta+\sin(n-1)\theta}{\sin\theta}\\ \frac{v_q}{V} &= -\frac{\pi^2}{24\lambda^2}\sin 2\beta\cdot b_1\end{aligned}\right\}\quad(24)$$

Therefore, by the following boundary conditions

$$\frac{dy_c}{dx}=\alpha-\frac{v_\gamma+v_q}{V}\,,\quad(25)$$

the unknown coefficient A_n can be determined as follows;

$$\left.\begin{aligned}A_0 &= \frac{\alpha+c_0+\dfrac{\pi^2}{48\lambda^2}\cos 2\beta\cdot c_2-\dfrac{\pi^2}{24\lambda^2}\sin 2\beta\cdot b_1}{1+\dfrac{\pi^2}{24\lambda^2}\cos 2\beta}\\ A_1 &= \frac{c_1-\dfrac{\pi^2}{12\lambda^2}\cos 2\beta\cdot A_0}{1+\dfrac{\pi^2}{24\lambda^2}\cos 2\beta}\\ A_2 &= c_2\\ A_3 &= c_3\\ &\cdots\cdots\cdots\cdots\end{aligned}\right\}\quad(26)$$

The other coefficients B_n can also be determined by the relation; $w_d=u_\gamma+u_q$, as follows;

$$\begin{aligned}B_1 &= -\frac{\pi^2}{24\lambda^2}\sin 2\beta\cdot\left(A_0-\frac{A_2}{2}\right)+\left\{1-\frac{\pi^2}{24\lambda^2}\sin 2\beta\cdot\left(A_0-\frac{A_2}{2}\right)+\frac{\pi^2}{24\lambda^2}\cos 2\beta\right\}\cdot b_1\\ &\quad-\frac{\pi^2}{24\lambda^2}\sin 2\beta\cdot\left(A_0+\frac{A_1}{2}\right)\cdot 2b_2\\ B_2 &= -\frac{\pi^2}{24\lambda^2}\sin 2\beta\cdot\left(A_0+\frac{A_1}{2}\right)+\left\{1-\frac{\pi^2}{24\lambda^2}\sin 2\beta\left(A_0-\frac{A_2}{2}\right)\right\}\cdot 2b_2\\ &\quad-\frac{\pi^2}{24\lambda^2}\sin 2\beta\cdot\left(A_0+\frac{A_1}{2}\right)\cdot(b_1+3b_3)\end{aligned}$$

$$\left.\begin{aligned}B_3 &= \left\{1-\frac{\pi^2}{24\lambda^2}\sin 2\beta\cdot\left(A_0-\frac{A_2}{2}\right)\right\}\cdot 3b_3 \\ &\quad -\frac{\pi^2}{24\lambda^2}\sin 2\beta\cdot\left(A_0+\frac{A_1}{2}\right)(2b_2+4b_4) \\ B_4 &= \left\{1-\frac{\pi^2}{24\lambda^2}\sin 2\beta\cdot\left(A_0-\frac{A_2}{2}\right)\right\}\cdot 4b_4 \\ &\quad -\frac{\pi^2}{24\lambda^2}\sin 2\beta\cdot\left(A_0+\frac{A_1}{2}\right)(3b_3+5b_5) \\ &\cdots\cdots\cdots\cdots\cdots\cdots\cdots .\end{aligned}\right\} \tag{27}$$

Thus, the velocity and pressure distributions along the surface can be calculated by the above obtained coefficients, A_n and B_n, and the circulation Γ is determined as follows;

$$\frac{\Gamma}{Vc} = \pi\left(A_0+\frac{A_1}{2}\right) \tag{28}$$

6. Induced Velocities due to Tunnel Wall

Now, let the induced velocities along the airfoil due to the tunnel walls u_w and v_w, and assume that the induced velocities u_w and v_w are generally smaller than the ones, u_γ, v_γ, u_q and v_q, due to the neighbouring airfoils. Therefore, each airfoil in the cascade may be replaced by the single vortex with the circulation Γ at the 1/4-chord point on the chord, and neglect the effects due to the doublet which expresses the thickness of airfoil. Then the induced velocities u_w and v_w can be determined by the following equation;

$$u_w - iv_w = \frac{dF_1}{d\zeta}\frac{d\zeta}{dz} - \frac{dF_2}{dz}, \tag{29}$$

where F_1 is the complex potential function (7) shown in Part I, and F_2 is a complex potential function as follows;

$$F_2(z) = -\frac{i\Gamma}{2\pi}\log\sinh\left\{\frac{\pi}{d}\bar{e}^{i\beta_1}\left(z-\frac{c}{4}\right)\right\} + \lim_{a\to\infty}\left(\frac{i\Gamma}{2\pi}\right)\log\sinh\left\{\frac{\pi}{d}\bar{e}^{i\beta_1}(z-a)\right\}. \tag{30}$$

The second term of eq. (30) represents the flow in the case when the trailing vorticies from each airfoil in the cascade flow away infinitely.

Now, express the induced velocities, u_w and v_w, along the chord as follows;

$$u_w - iv_w = (u_{w_0} - iv_{w_0}) + (u_{w_1} - iv_{w_1})\, x, \tag{31}$$

where u_{w_0} and v_{w_0} are the velocity components and u_{w_1} and v_{w_1} the velocity gradient components at the considered point on the chord. These induced velocities due to the m-th airfoil can be given at the neighbourhood of the n-th airfoil by an approximate calculation;

$$
\begin{aligned}
\frac{u_{w_0}}{V} &= \frac{\Gamma}{2VH}\left\{\frac{E_1}{2\xi}-\frac{D_1E_2-E_1D_2}{D^2+E_1^2}\right\}+\frac{\Gamma}{2VH}\left\{-E_1\sum{}' f_1(\xi,\eta)+D_1\sum{}' f_2(\xi,\eta)\right\} \\
&\quad -\frac{\Gamma}{VH}\sum\left(\frac{\Delta\Gamma}{\Gamma}\right)\frac{\eta+\tan\beta_1}{\xi^2+(\eta+\tan\beta_1)^2}+\frac{\sin\beta_1}{2\lambda}\left(\frac{\Gamma}{Vc}\right) \\
\frac{v_{w_0}}{V} &= \frac{\Gamma}{2VH}\left\{\frac{D_1}{2\xi}-\frac{D_1D_2+E_1E_2}{D_1^2+E_1^2}\right\}-\frac{\Gamma}{2VH}\left\{D_1\sum{}' f_1(\xi,\eta)+E_1\sum{}' f_2(\xi,\eta)\right\} \\
&\quad +\frac{V}{VH}\sum{}'\left(\frac{\Delta\Gamma'}{\Gamma}\right)\frac{\xi}{\xi^2(\eta+\tan\beta_1)^2}-\frac{\cos\beta_1}{2\lambda}\left(\frac{\Gamma}{Vc}\right) \\
\frac{u_{w_1}}{V} &= \frac{\pi\Gamma}{4VH^2}\left\{\frac{D_1E_1}{\xi}-E_2+F_1\right\}\frac{1}{\xi}+\frac{\pi\Gamma}{VH^2}\sum\left(\frac{\Delta\Gamma}{\Gamma}\right)E_2+\frac{\pi\Gamma}{6Vd^2}\sin 2\beta_1 \\
&\quad +\frac{\pi\Gamma}{2VH^2}\{\{D_2E_3+D_3E_2)\sum{}' f_1(\xi,\eta)-(D_2D_3-E_2E_3)\sum{}' f_2(\xi,\eta)\} \\
&\quad -\frac{\pi\Gamma}{VH^2}\{D_1E_1\sum{}' g_1(\xi,\eta)-(D_1^2-E_1^2)\sum{}' g_2(\xi,\eta)\} \\
\frac{v_{w_1}}{V} &= \frac{\pi\Gamma}{4VH^2}\left\{\frac{D_1^2-E_1^2}{2\xi}-D_2+F_2\right\}\frac{1}{\xi}+\frac{\pi\Gamma'}{VH^2}\sum\left(\frac{\Delta\Gamma}{\Gamma}\right)D_2-\frac{\pi\Gamma}{6d^2}\cos 2\beta_1 \\
&\quad +\frac{\pi\Gamma}{2VH^2}\{(D_2D_3-E_2E_3)\sum{}' f_1'(\xi,\eta)+(D_2E_3+D_3E_2)\sum{}' f_2(\xi\ \eta)\} \\
&\quad -\frac{\pi\Gamma}{2VH^2}\{(D_1^2-E_1^2)\sum{}' g_1(\xi,\eta)+4D_1E_1\sum{}' g_2(\xi,\eta)\}\,, \qquad (32)
\end{aligned}
$$

where

$$
D_1=\xi\left[1-\frac{\sec^2\beta_1}{\xi^2+(\eta+\tan\beta_1)^2}\right], \qquad E_1=\eta-\tan\beta_1+\frac{(\eta+\tan\beta_1)\sec^2\beta_1}{\xi^2+(\eta+\tan\beta_1)^2}
$$

$$
D_2=\frac{D_1[\xi^2+(\eta\tan\beta_1)^2]+2E_1\xi(\eta+\tan\beta_1)}{[\xi^2+(\eta+\tan\beta_1)^2]^3}, \qquad E_2=\frac{E_1[\xi^2+(\eta+\tan\beta_1)^2]-2D_1\xi(\eta+\tan\beta_1)}{[\xi^2+(\eta+\tan\beta_1)^2]^3}
$$

$$
D_3=\xi^2+\eta^2-1-2\tan\beta_1\cdot\eta\,, \qquad E_3=2\xi(\eta+\tan\beta_1)
$$

$$
F_1=\frac{(2E_1\xi-E_2)\,\xi-(2D_1\xi-D_2)(\eta+\tan\beta_1)}{\xi^2+(\eta+\tan\beta_1)^2},
$$

$$
F_2=\frac{(2D_1\xi-D_2)\,\xi+(2E_1\xi-E_2)(\eta+\tan\beta_1)}{\xi^2+(\eta+\tan\beta_1)^2},
$$

and

$$
\begin{aligned}
f_1(\xi,\eta) &= \frac{\xi-\xi_m}{(\xi-\xi_m)^2+(\eta-\eta_m)^2}-\frac{\xi+\xi_m}{(\xi+\xi_m)^2+(\eta-\eta_m)^2}, \qquad (33) \\
f_2(\xi,\eta) &= \frac{\eta-\eta_m}{(\xi-\xi_m)^2+(\eta-\eta_m)^2}-\frac{\eta+\eta_m}{(\xi+\xi_m)^2+(\eta-\eta_m)^2}, \\
g_1(\xi,\eta) &= \frac{(\xi-\xi_m)^2-(\eta-\eta_m)^2}{\{(\xi-\xi_m)^2+(\eta-\eta_m)^2\}^2}-\frac{(\xi+\xi_m)^2-(\eta-\eta_m)^2}{\{(\xi+\xi_m)^2+(\eta-\eta_m)^2\}^2}, \\
g_2(\xi,\eta) &= \frac{(\xi-\xi_m)(\eta-\eta_m)}{\{(\xi-\xi_m)^2+(\eta-\eta_m)^2\}^2}-\frac{(\xi-\xi_m)(\eta-\eta_m)}{\{(\xi+\xi_m)^2+(\eta-\eta_m)^2\}^2},
\end{aligned}
$$

and then $\xi=\kappa\cos\gamma$, $\eta=\kappa\sin\gamma$ and $\sum{}'$ denotes the summation except the airfoil considered, and the suffix m the corresponding values of the m-th airfoil. It should be noticed here that the sign of the induced velocities and velocity gradients is opposite to the ones obtained by the eq. (32), with the reference to the co-ordinate axes, as shown in Fig. 7.

7. Thin Airfoil Theory of Cascade under Tunnel Wall Interference

As the above obtained velocities and velocity gradients are of various magnitudes at the positions of each airfoil in the cascade, the distributions of circulation along the chord become unequal to each other. Then, put the additional circulation distribution $\Delta\gamma$ due to the wall interference into the following expression;

$$\frac{\Delta\gamma}{2V} = \Delta A_0 \tan\frac{\theta}{2} + \sum_{n=1}^{\infty} \Delta A_n \sin n\theta\,, \tag{34}$$

then the additional circulation $\delta\Gamma$ becomes as

$$\frac{\delta\Gamma}{Vc} = \pi\left(\Delta A_0 + \frac{\Delta A_1}{2}\right). \tag{35}$$

then induced velocities due to the obove odditional circulation $\delta\Gamma$ are similarly given by the methods of the paragraph 5 as follows;

$$\left.\begin{aligned} \frac{\Delta u_\gamma}{V} &= -\frac{\pi\cos\beta}{2Z\lambda}\sum{}'\cot\left(\frac{m\pi}{Z}\right)\cdot\left(\Delta A_0+\frac{\Delta A_1}{2}\right) \\ \frac{\Delta v_\gamma}{V} &= -\Delta A_0 - \sum_{n=1}^{\infty}\Delta A_n\cdot\cos n\theta \\ &\quad + \frac{\pi\sin\beta}{2Z\lambda}\sum{}'\cot\left(\frac{m\pi}{Z}\right)\cdot\left(\Delta A_0+\frac{\Delta A_1}{2}\right), \end{aligned}\right\} \tag{36}$$

where $m=0, \pm1, \pm2, \pm3, \cdots$ and $\sum{}'$ enotes the summation excepting $m=0$. Similarly the induced velocities due to the source-sink distribution become as

$$\left.\begin{aligned} \frac{\Delta u_q}{V} &= \left(\frac{u_{w0}}{V}+\frac{\Delta u_\gamma}{V}\right)\left\{\sum_{n=1}^{\infty} nb_n\frac{\sin n\theta}{\sin\theta}+\frac{\pi^2}{24\lambda^2}\cos 2\beta\cdot b_1\right\} \\ &\quad + \left(\frac{u_{w1}}{V}\right)\left\{\sum_{n=1}^{\infty} nb_n\frac{\sin(n+1)\theta+\sin(n-1)\theta}{\sin\theta}-\frac{\pi^2}{12\lambda^2}\cos 2\beta\cdot b_1\right\}, \\ \frac{\Delta v_q}{V} &= -\left(\frac{u_{w0}}{V}+\frac{\Delta u_\gamma}{V}\right)\frac{\pi^2}{24\lambda^2}\sin 2\beta\cdot b_1 \\ &\quad + \left(\frac{u_{w1}}{V}\right)\frac{\pi^2}{24\lambda^2}\sin 2\beta\cdot b_2\,. \end{aligned}\right\} \tag{37}$$

The induced velocities due to the additional distribution on each airfoil and the induced velocities due to the wall interference should satisfy the boundary condition on the surface of each airfoil. Thus the unknown coefficients ΔA_n can be determined as follows;

$$\left.\begin{aligned} \Delta A_0 &= \frac{u_{w0}}{V}-\frac{\pi^2}{24\lambda^2}\sin 2\beta\cdot\left\{b_1\left(\frac{u_{w0}}{V}\right)-b_2\left(\frac{u_{w1}}{V}\right)\right\} \\ &\quad + \frac{\sin\beta}{2Z\lambda}\left\{1+\frac{\pi^2}{24\lambda^2}\sin 2\beta\cdot b_1\right\}\sum{}'\left(\frac{\delta\Gamma}{Vc}\right)\cot\left(\frac{m\pi}{Z}\right) \\ \Delta A_1 &= \frac{v_{w0}}{V} \\ \Delta A_2 &= \Delta A_3 = \cdots = 0\,. \end{aligned}\right\} \tag{38}$$

Accordingly, the additional quantities ΔB_n for the velocity increments due to the thickness are given as follows;

$$\left.\begin{aligned}
\Delta B_1 &= \left(\frac{u_{w_0}}{V}+\frac{\Delta u_\gamma}{V}\right)\left\{1+\left(1+\frac{\pi^2}{24\lambda^2}\cos 2\beta\right)\cdot b_1\right\}\\
&\quad+\left(\frac{u_{w_1}}{V}\right)\left(2b_2-\frac{\pi^2}{12\lambda^2}\cos 2\beta\cdot b_1\right)\\
&\quad-\frac{\pi\cos\beta}{2Z\lambda}\sum{}'\left(\Delta A_0+\frac{\Delta A_1}{2}\right)\cot\frac{m\pi}{Z}\\
\Delta B_2 &= \frac{1}{2}\left(\frac{u_{w_1}}{V}\right)+\left(\frac{u_{w_1}}{V}\right)(b_1+3b_3)+\left(\frac{u_{w_0}}{V}+\frac{\Delta u_\gamma}{V}\right)\cdot 2b_2\\
\Delta B_3 &= \left(\frac{u_{w_1}}{V}\right)(2b_2+4b_4)+\left(\frac{u_{w_0}}{V}+\frac{\Delta u_\gamma}{V}\right)\cdot 3b_3\\
\Delta B_4 &= \left(\frac{u_{w_1}}{V}\right)(3b_3+5b_5)+\left(\frac{u_{w_0}}{V}+\frac{\Delta u_\gamma}{V}\right)\cdot 4b_4\\
&\cdots\cdots\cdots\cdots\cdots\cdots\cdots\cdots .
\end{aligned}\right\}\tag{39}$$

Inserting the coefficients ΔA_0 and ΔA_1 of the eq. (38) into the eq. (35), the following equation is obtained;

$$\begin{aligned}
&\left(\frac{\delta\Gamma}{Vc}\right)-\frac{\pi\sin\beta}{2Z\lambda}\left\{1+\frac{\pi^2}{24\lambda^2}\sin 2\beta\cdot b_1\right\}\sum{}'\cot\left(\frac{m\pi}{Z}\right)\cdot\left(\frac{\delta\Gamma}{Vc}\right)\\
&=\pi\left[\left(\frac{u_{w_0}}{V}\right)+\frac{1}{2}\left(\frac{u_{w_1}}{V}\right)-\frac{\pi^2}{24\lambda^2}\sin 2\beta\cdot\left\{b_1\left(\frac{u_{w_0}}{V}\right)-b_2\left(\frac{u_{w_1}}{V}\right)\right\}\right]
\end{aligned}\tag{40}$$

As the eq. (40) can be on each airfoil in the cascade, the Z linear simultanous equations of $\delta\Gamma/Vc$ are obtained. Hence the increments of circulation $\delta\Gamma/Vc$ can be given by the above-mentioned simultanous equations and, consequently, the additional distributions of circulation can be also calculated.

Now, the above calculation was performed under the induced velocities due to the wall interference assuming that each airfoil in the cascade has the same magnitude of circulation. Hence, the increments obtained above of circulation $\delta\Gamma/Vc$ give again the small change of the induced velocities and velocity gradients obtained above, and the changes denoted respectively as Δu_{w_0}, Δv_{w_0}, Δu_{w_1} and Δv_{w_1}, are obtained as follows;

$$\begin{aligned}
\frac{\Delta u_{w_0}}{V} &= \frac{c}{2H}\left(\frac{\delta\Gamma}{Vc}\right)\left\{\frac{\boldsymbol{E}_1}{2\xi}-\frac{\boldsymbol{D}_1\boldsymbol{E}_2-\boldsymbol{D}_2\boldsymbol{E}_1}{\boldsymbol{D}_1^2+\boldsymbol{E}_1^2}\right\}\\
&\quad+\frac{c}{2H}\left\{-\boldsymbol{E}_1\sum{}'\left(\frac{\delta\Gamma}{Vc}\right)\mathbf{f}_1(\xi,\eta)+\boldsymbol{D}_1\sum{}'\left(\frac{\delta\Gamma}{Vc}\right)f_2(\xi,\eta)\right\}\\
&\quad-\frac{c}{2H}\sum\left(\frac{\delta\Gamma}{Vc}\right)\left(\frac{\Delta\Gamma}{\Gamma}\right)\frac{\eta+\tan\beta_1}{\xi^2+(\eta+\tan\beta_1)^2}\\
&\quad+\frac{c}{H}\left\{\sin\beta_1\cdot\cos\beta_1\sum\left(\frac{\delta\Gamma}{Vc}\right)-\pi\cos^2\beta_1\sum{}'\left(\frac{\delta\Gamma}{Vc}\right)\cot\left(\frac{m\pi}{Z}\right)\right.
\end{aligned}$$

$$\frac{\Delta u_{w_0}}{V}=\frac{c}{2H}\left(\frac{\delta\Gamma}{Vc}\right)\left\{\frac{D_1}{2\xi}-\frac{D_1D_2+E_1E_2}{D_1^2+E_1^2}\right\}$$
$$-\frac{c}{2H}\left\{D_1\sum{}'\left(\frac{\delta\Gamma}{Vc}\right)f_1(\xi,\eta)+E_1\sum{}'\left(\frac{\delta\Gamma}{Vc}\right)f_2(\xi,\eta)\right\}$$
$$+\frac{c}{2H}\sum\left(\frac{\delta\Gamma}{Vc}\right)\left(\frac{\Delta\Gamma}{\Gamma}\right)\frac{\xi}{\xi^2+(\eta+\tan\beta_1)^2}$$
$$-\frac{c}{H}\left\{\cos^2\beta_1\sum\left(\frac{\delta\Gamma}{Vc}\right)+\pi\cos\beta_1\cdot\sin\beta_1\sum{}'\left(\frac{\delta\Gamma}{Vc}\right)\cot\left(\frac{m\pi}{Z}\right)\right\}$$
$$\frac{\Delta u_{w_1}}{V}=\frac{\pi c}{4H^2}\left(\frac{\delta\Gamma}{Vc}\right)\left\{\frac{D_1E_1}{\xi}-E_2+F_1\right\}\frac{1}{\xi}\tag{41}$$
$$+\frac{\pi c}{2H^2}\left\{(D_2E_3+D_3E_2)\sum{}'\left(\frac{\delta\Gamma}{Vc}\right)f_1(\xi,\eta)-(D_2D_3-E_2E_3)\sum{}'\left(\frac{\delta\Gamma}{Vc}\right)f_2(\xi,\eta)\right\}$$
$$-\frac{\pi c}{H^2}\left\{D_1E_1\sum{}'\left(\frac{\delta\Gamma}{Vc}\right)g_1(\xi,\eta)-(D_1^2-E_1^2)\sum{}'\left(\frac{\delta\Gamma}{Vc}\right)g_2(\xi,\eta)\right\}$$
$$+\frac{\pi c}{H^2}\sum\left(\frac{\delta\Gamma}{Vc}\right)\left(\frac{\Delta\Gamma}{\Gamma}\right)E_2+\frac{\pi^2c}{2H^2}\sin 2\beta_1\cos^2\beta_1\sum{}'\left(\frac{\delta\Gamma}{Vc}\right)\operatorname{cosec}^2\left(\frac{m\pi}{Z}\right)$$
$$\frac{\Delta v_{w_1}}{V}=\frac{\pi c}{4H^2}\left(\frac{\delta\Gamma}{Vc}\right)\left\{\frac{D_1^2-E_1^2}{\xi}-D_2+F_2\right\}\frac{1}{\xi}$$
$$+\frac{\pi c}{2H^2}\left\{(D_2D_3+E_2E_3)\sum{}'\left(\frac{\delta\Gamma}{Vc}\right)f_1(\xi,\eta)+(D_2E_3+D_3E_2)\sum{}'\left(\frac{\delta\Gamma}{Vc}\right)f_2(\xi,\eta)\right\}$$
$$-\frac{\pi c}{H^2}\left\{(D_1^2-E_1^2)\sum{}'\left(\frac{\delta\Gamma}{Vc}\right)g_1(\xi,\eta)+4D_1E_1\sum{}'\left(\frac{\delta\Gamma}{Vc}\right)g_2(\xi,\eta)\right\}$$
$$-\frac{\pi c}{H^2}\sum\left(\frac{\delta\Gamma}{Vc}\right)\left(\frac{\Delta\Gamma}{\Gamma}\right)D_2-\frac{\pi^2c}{2H^2}\cos 2\beta_1\cos^2\beta_1\sum{}'\left(\frac{\delta\Gamma}{Vc}\right)\operatorname{cosec}^2\left(\frac{m\pi}{Z}\right)$$

Further, the additional distributions of circulation due to the changes of induced velocities obtained above are assumed as follows;

$$\frac{\Delta\gamma'}{2V}=\Delta A_0'\tan\frac{\theta}{2}+\sum_{n=1}^{\infty}\Delta A'_n\sin n\theta\tag{42}$$

and the change of circulation $(\delta\Gamma/Vc)'$ becomes as

$$\left(\frac{\delta\Gamma}{Vc}\right)'=\pi\left(\Delta A_0'+\frac{\Delta A_1'}{2}\right).\tag{43}$$

Hence, the induced velocities and velocity gradients are given as follows;

$$\left.\begin{aligned}\frac{\Delta u_\gamma'}{V}&=-\frac{\pi\cos\beta}{2Z\lambda}\sum{}'\cot\left(\frac{m\pi}{Z}\right)\left(\Delta A_0'+\frac{\Delta A_1'}{2}\right)\\\frac{\Delta v_\gamma'}{V}&=-\Delta A_0'-\sum_{n=1}^{\infty}\Delta A_n'\cos n\theta+\frac{\pi\sin\beta}{2Z\lambda}\sum{}'\cot\left(\frac{m\pi}{Z}\right)\left(\Delta A_0'+\frac{\Delta A_1'}{2}\right)\end{aligned}\right\}\tag{44}$$

and

$$\left.\begin{aligned}\frac{\Delta u_q'}{V}&=\left(\frac{\Delta u_{w_0}}{V}\right)\left\{\sum_{n=1}^{\infty}nb_n\frac{\sin n\theta}{\sin\theta}+\frac{\pi^2}{24\lambda^2}\cos 2\beta\cdot b_1\right\}\\&\quad+\left(\frac{\Delta u_{w_1}}{V}\right)\left\{\sum_{n=1}^{\infty}nb_n\frac{\sin(n+1)\theta+\sin(n-1)\theta}{\sin\theta}-\frac{\pi^2}{12\lambda^2}\cos 2\beta\cdot b_1\right\}\\\frac{\Delta v_q'}{V}&=-\left(\frac{\Delta u_{w_0}}{V}\right)\frac{\pi^2}{24\lambda^2}\sin 2\beta\cdot b_1+\left(\frac{\Delta u_{w_1}}{V}\right)\frac{\pi^2}{24\lambda^2}\sin 2\beta\cdot b_2\end{aligned}\right\}\tag{45}$$

Therefore, the coefficients $\Delta A_n'$ and $\Delta B_n'$ are similarly given as follows;

$$\begin{aligned}\Delta A_0' &= \frac{\pi \sin\beta}{2Z\lambda}\sum{}' \cot\left(\frac{m\pi}{Z}\right)\left(\Delta A_0' + \frac{\Delta A_1'}{2}\right)\\ &\quad -\frac{\pi^2}{24\lambda^2}\sin 2\beta\cdot\left\{b_1\left(\frac{\Delta u_{w_0}}{V}\right) - b_2\left(\frac{\Delta u_{w_1}}{V}\right)\right\} + \frac{\Delta u_{w_0}}{V}\\ \Delta A_1' &= \frac{\Delta u_{w_1}}{V}\\ \Delta A_2' &= \Delta A_3' = \cdots = 0\end{aligned} \tag{46}$$

and

$$\begin{aligned}\Delta B_1' &= -\frac{\pi \cos\beta}{2Z\lambda}\sum{}' \cot\left(\frac{m\pi}{Z}\right)\left(\Delta A_0' + \frac{\Delta A_1'}{2}\right)\\ &\quad + \left(\frac{\Delta u_{w_0}}{V}\right)\left(1 + \frac{\pi^2}{24\lambda^2}\cos 2\beta\right)\cdot b + \left(\frac{\Delta u_{w_1}}{V}\right)\left(2b_2 - \frac{\pi^2}{12\lambda^2}\cos 2\beta\cdot b_1\right) + \frac{\Delta u_{w_0}}{V}\\ \Delta B_2' &= \left(\frac{\Delta u_{w_0}}{V}\right)\cdot 2b_2 + \left(\frac{\Delta u_{w_1}}{V}\right)(b_1 + 3b_3) + \frac{1}{2}\left(\frac{\Delta u_{w_1}}{V}\right)\\ \Delta B_3' &= \left(\frac{\Delta u_{w_0}}{V}\right)\cdot 3b_3 + \left(\frac{\Delta u_{w_1}}{V}\right)(2b_2 + 4b_4)\\ \Delta B_4' &= \left(\frac{\Delta u_{w_0}}{V}\right)\cdot 4b_3 + \left(\frac{\Delta u_{w_1}}{V}\right)(3b_3 + 5b_5)\\ &\cdots\cdots\cdots\cdots\end{aligned} \tag{47}$$

Consequently, the following equation is similarly obtained;

$$\begin{aligned}&\left(\frac{\delta\Gamma}{Vc}\right)' - \frac{\pi\sin\beta}{2Z\lambda}\sum{}'\left(\frac{\delta\Gamma}{Vc}\right)'\cot\left(\frac{m\pi}{Z}\right)\\ &= \frac{\Delta u_{w_0}}{V} + \frac{1}{2}\frac{\Delta u_{w_1}}{V} - \frac{\pi^2}{24\lambda^2}\sin 2\beta\left\{b_1\frac{\Delta u_{w_0}}{V} - b_2\frac{\Delta u_{w_1}}{V}\right\},\end{aligned} \tag{48}$$

The roots of the Z linear simultanous equations (48) give the additional circulation $(\delta\Gamma/Vc)'$.

Calculating the induced velocities due to the tunnel walls by means of $(\delta\Gamma/Vc)'$, the ones obtained above, and repeating the above-mentioned calculation, the additional circulation $(\delta\Gamma/Vc)''$ and coefficents $\Delta A_n''$ and $\Delta B_n''$ can be determined. Thus the same procedures can be applied to the following approximation successively.

8. Procedures of Calculation and some Numerical and Experimental Examples

Suppose a cascade composed of $Z=2(N+1)$ or $2N+1$ airfoils having the given shape under the cascade conditions of β and λ. In the tunnel test, the inlet velocity V_1 at the inlet of cascade and the incidence angle α_1 to V_1 are known, but the mean velocity V and incidence angle α to V are not yet known. Given the turning angle θ, the unknown quantities V and α can be determined by the following relations;

$$\left.\begin{aligned}\tan(\beta_1-\Delta\theta) &= \sin(2\beta_1-\theta)/2\cos\beta_1\cos(\beta_1-\theta)\\ \beta_1 &= \beta+\alpha_1, \qquad \Delta\theta=\alpha_1-\alpha\\ \frac{V}{V_1} &= \sqrt{\sin^2(2\beta-\theta)+4\cos^2\beta_1\cos^2(\beta_1-\theta)}/2\cos(\beta_1-\theta)\,.\end{aligned}\right\} \qquad (49)$$

Firstly, assume the turning angle θ and determine the mean velocity V and incidence angle α by means of the eq. (49). Then the coefficients A_n and B_n and the circulation Γ can be calculated by the methods developed in the paragraph 7, neglecting the wall interference and assuming the circulation to be equal to each airfoil. Let the values of A_n, B_n and Γ be the solution of the zero order approximation.

Next, determine the induced velocities due to the tunnel wall interference from the solutions of zero order approximation by means of the equations in the paragraph 8, and then the additional coefficients ΔA_n and ΔB_n and the additional circulation $(\delta\Gamma/Vc)$ can be calculated. Let the values, as above obtained, be the additional ones of the first order approximation.

Further performing the same procedures from the first order approximate solutions, the additional coefficients $\Delta A_n'$ and $\Delta B_n'$ and additional circulation $(\delta\Gamma/Vc)'$ can be calculated as the second order approximate solutions. Repeating the same procedures until the additional quantities of ΔA_n^ν, ΔB_n^ν and $(\delta\Gamma/Vc)^\nu$ become negligibly small, the circulation of each airfoil in the cascade can be determined; and then the turning angle θ can be given by the eq. (17) with the above obtained values of circulation. Finally, examine the angle θ thus obtained to see if it is equal to the first assumed value or not.

For example, the calculation was performed, as shown in Fig. 8, in the case of the cascade, which is composed of N.A.C.A. 6409, under the conditions of $Z=5$, $\beta_1=40$, $\lambda=1$ and $\alpha_1=0°$. The processes of calculation are shown in the Table I, and the numerical values in the case of the cascade without the tunnel wall interference are also

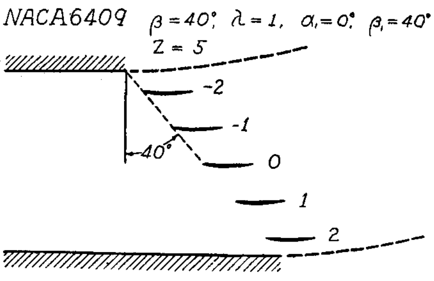

Fig. 8

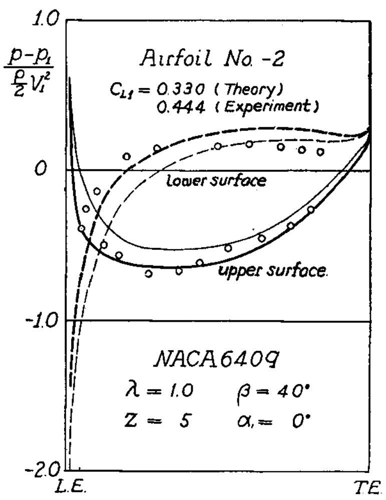

Fig. 9-a

shown within the bracket in the Table I in order to show the effects of wall interference. Fig. 9 shows the pressure distribution along the chord of each airfoil, the thick lines are ones influenced by the wall interference and the thin lines the ones without the interference. On the other hand, the experiments of the same cascade with the same conditions, as shown in the numerical examples, was performed. The tested cascade is so constructed that the pressure distribution of each airfoil

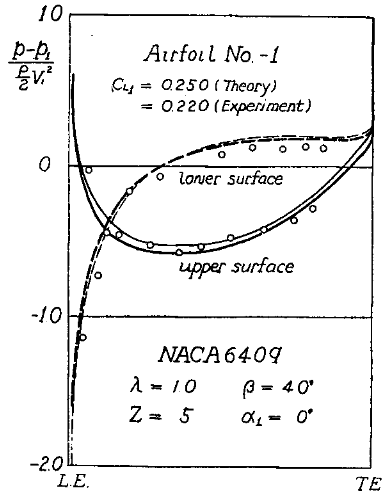

Fig. 9-b

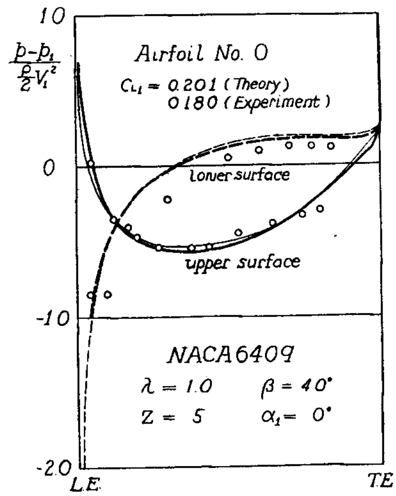

Fig. 9-c

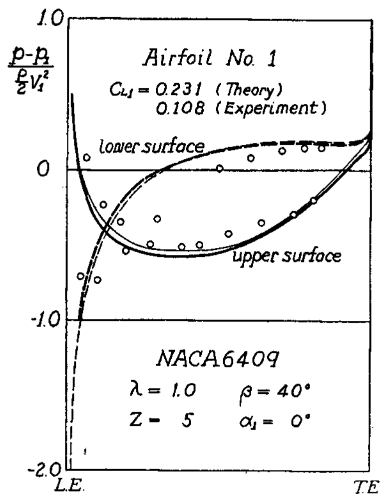

Fig. 9-d

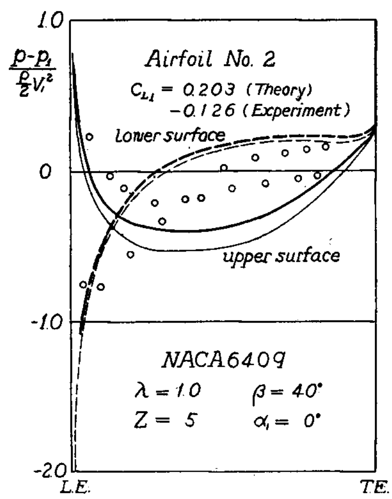

Fig. 9-e

Table I

	θ	assumed	5° 48′	(5° 14′)
Zero Order Approximation	α	(49)	$-2°$ 47′	($-2°$ 31′)
	V/V_1		0.9618	(0.9652)
	Γ/VC	(28)	0.0996	(0.1150)
	Γ/V_1C	(49)	0.0958	(0.1110)
	A_0	(26)	−0.0884	(−0.0833)
	A_1		0.2403	(0.2397)
	A_2		−0.0524	(−0.0524)
	A_3		0.0024	(0.0024)
	A_4		−0.0140	(−0.0140)
	A_5		0.0024	(0.0024)
	B_1	(27)	0.1119	(0.1097)
	B_2		−0.0739	(−0.0759)
	B_3		−0.0026	(−0.0026)
	B_4		−0.0053	(−0.0073)
	B_5		−0.0021	(−0.0021)

NACA 6409

β = 40° $\lambda = 1$
$\alpha_1 = 0°$ $Z = 5$

a_0	0.0607	b_4	−0.0018
a_1	−0.0067	b_5	−0.0004
a_2	−0.0053	b_6	−0.0003
a_3	0.0064		
a_4	−0.0006		
a_5	0.0014	c_0	−0.0195
a_6	0.0002	c_1	0.2636
		c_2	−0.0524
		c_3	0.0024
b_1	0.0783	c_4	−0.0140
b_2	−0.0293	c_5	0.0024
b_3	−0.0012		

	No.		−2	−1	0	1	2
First Order Approximation	u_{w0}/V	(32)	0.0055	0.0112	0.0081	0.0117	−0.0138
	v_{w0}/V		0.0164	0.0131	0.0052	0.0065	0.0041
	u_{w1}/V		0.0013	0.0026	0.0039	0.0019	−0.0013
	v_{w1}/V		−0.0047	0.0029	0.0017	0.0014	−0.0116
	$(\delta\Gamma/Vc)$	(40)	0.0553	0.0355	0.0109	0.0238	0.0065
	ΔA_0	(38)	0.0191	0.0098	0.0026	0.0069	−0.0037
	ΔA_1		−0.0048	0.0030	0.0018	0.0014	−0.0116
	ΔB_1	(39)	0.0002	0.0211	0.0133	0.0126	−0.0226
	ΔB_2		0.0009	0.0000	0.0013	0.0004	0.0008
	ΔB_3		−0.0001	−0.0003	−0.0003	0.0000	0.0002
	ΔB_4		0.0000	−0.0002	0.0000	0.0000	0.0002
	ΔB_5		0.0000	0.0000	0.0000	0.0000	0.0000
Second Order Approximation	$\Delta u_{w0}/V$	(41)	0.0010	0.0033	−0.0003	0.0007	−0.0035
	$\Delta v_{w0}/V$		0.0074	0.0029	−0.0003	−0.0003	−0.0001
	$\Delta u_{w1}/V$		−0.0014	0.0016	0.0004	0.0001	−0.0008
	$\Delta v_{w1}/V$		0.0018	0.0006	0.0002	−0.0007	−0.0033
	$(\delta\Gamma/Vc)'$	(48)	0.0249	0.0000	−0.0018	0.0016	0.0036
	$\Delta A_0'$	(46)	0.0070	−0.0003	−0.0007	0.0009	0.0028
	$\Delta A_1'$		0.0018	0.0006	0.0002	−0.0004	−0.0034
	$\Delta B_1'$	(47)	0.0017	0.0063	0.0001	−0.0004	−0.0067
	$\Delta B_2'$		−0.0008	0.0009	0.0002	0.0001	−0.0005
	$\Delta B_3'$		0.0000	0.0000	0.0000	0.0000	0.0000
	$\Delta B_4'$		0.0000	0.0000	0.0000	0.0000	0.0000
	$\Delta B_5'$		0.0000	0.0000	0.0000	0.0000	0.0000
		(13) (15)	5° 48′ (5° 14) from (16)				

can be measured, as shown in Fig. 10. The measured pressure distributions are plotted to the corresponding figures Fig. 8, and the lift-coefficients are also shown for the purpose of comparing the experimental results with the theoretical ones.

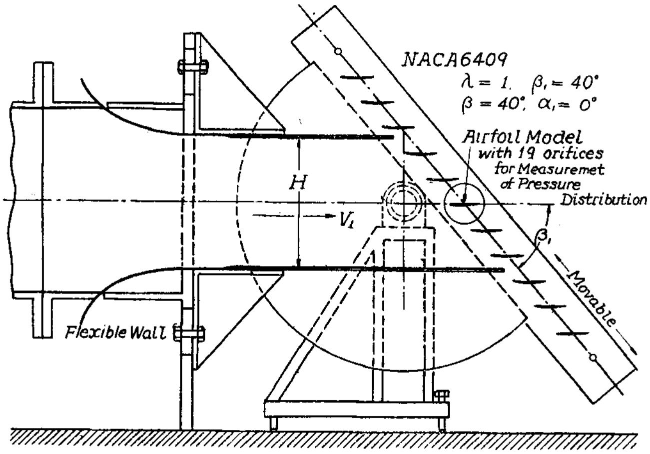

Fig. 10

Part III
Effects of Wall Boundary Layer upon Turning Angle

9. Variations of Turning Angle due to Wall Boundary Layer Effects

Finally, let us discuss the effects of wall boundary layer upon the turning angle by means of the two-dimensional potential flow theory of cascade test in Part I. Now, assuming the imaginary source distribution along the walls instead of the boundary layers, the problem can be dealt with the potential flow theory.

Let the displacement thickness of the wall boundary layer be δ^* and the velocity distribution along the walls w, and then put an imaginary source distribution $q(x)$ along them, as shown in Fig. 11 so that they should represent the boundary layer as:

$$q(x) = w \frac{d\delta^*}{ax}, \tag{50}$$

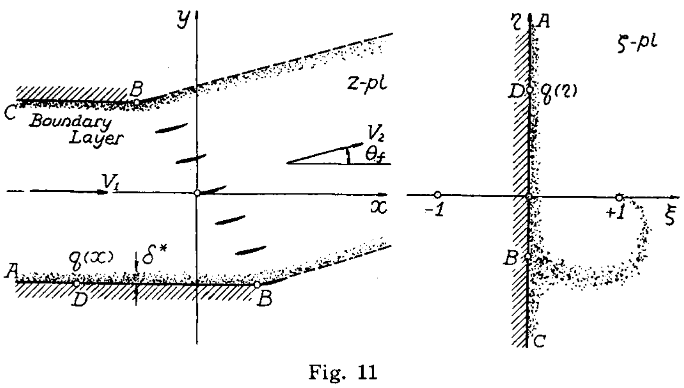

Fig. 11

where $d\delta^*/dx$ can be calculated by the boundary layer theory under the known velocity distribution along the walls. Using the mapping function in Part I, the corresponding source distribution $q(\eta)$ along the η-axis on the ζ-plane is given by

$$q(\eta) = q(x)\frac{dx}{d\eta} = w\frac{d\delta^*}{dx}\frac{dx}{d\eta}. \tag{51}$$

The velocity distribution w is given by the eq. (14), $dx/d\eta$ by the eq. (2) and $d\delta^*/dx$ by the boundary layer theory, then the above source distribution $q(\eta)$ can be evaluated by the eq. (51). Therefore, the induced velocity w_q at the point $\eta=\eta_1$ can be expressed as

$$w_q = \frac{1}{\pi}\int_{-\infty}^{\infty}\frac{q(\eta)}{\eta_1-\eta}d\eta. \tag{52}$$

Then, the induced velocity w_{qB} at B ($\eta_1=-\tan\beta_1$) is as follows;

$$w_{qB} = -\frac{1}{\pi}\int_{-\infty}^{\infty}\frac{q(\eta)}{\eta+\tan\beta_1}d\eta. \tag{53}$$

The imaginary flows from the imaginary source distributions flow out as the wakes into the downstream flow of cascade ($z=\infty$). As the point $z=\infty$ corresponds to the points $\zeta=\pm1$, the strength of sinks at the points $\zeta=\pm1$ must be

$$\int_A^B q(x)\,dx+\int_C^B q(q)\,dx = \int_A^B wd\delta^* + \int_C^B wd\delta^*.$$

Further, assuming that the velocity distribution w is nearly equal to the uniform velocity V_1 except near the edge points B and that the boundary layer thickness is negligibly small at the upstream walls (at A and C), the above mentioned strength of source is approximately expressed as

$$\int_A^B wd\delta^* + \int_C^B wd\delta^* \cong V_1(\delta^*_{Bl}+\delta^*_{Bu}) \equiv V_1\delta^*_B$$

where suffix u and l denote respectively the values of the upper and lower walls, and suffix B the values at the edge points B. Thus, the complex potential function $F_q(\zeta)$ due to the above sinks can be expressed by

$$F_q(\zeta) = \frac{i\Delta\Gamma_q}{2\pi}\log\frac{\zeta-1}{\zeta+1} - \frac{V_1\delta^*_B}{2\pi}\log(\zeta^2-1), \tag{54}$$

where $\Delta\Gamma_q$ is an unknown quantity of circulation at $\zeta=\pm1$ and can be determined as follows by the condition that the induced velocity w^*_{qB} at the point B, which is evaluated by the eq. (54), cansels the velocity w_{qB};

$$\frac{\Delta\Gamma_q}{V_1H} = \sec^2\beta_1\int_{-\infty}^{\infty}\frac{\frac{q(\eta)}{V_1H}}{\eta+\tan\beta_1}d\eta - \left(\frac{\delta^*_B}{H}\right)\tan\beta_1. \tag{55}$$

Hence, the velocities $u_{f\infty}$ and $v_{f\infty}$ along the x- and y-axis at the downstream of cascade are induced by the above sinks and circulations. As the results of some calculation, they become

$$\left.\begin{aligned}\frac{u_{f\infty}}{V_1} &= -\frac{\Delta\Gamma_q}{V_1 H}\sin\beta_1\cos\beta_1+\left(\frac{\delta_B^*}{H}\right)\cos^2\beta_1\\ \frac{v_{f\infty}}{V_1} &= -\frac{\Delta\Gamma_q}{V_1 H}\cos^2\beta_1+\left(\frac{\delta_B^*}{H}\right)\sin\beta_1\cos\beta_1\end{aligned}\right\} \tag{56}$$

Therefore, the turning angle θ_f under the wall boundary layer effects is as follows;

$$\tan\theta_f = \tan\theta\,\frac{1+\left(\frac{v_{f\infty}}{V_1}\right)\Big/\left(\frac{v_\infty}{V_1}\right)}{1+\left(\frac{u_{f\infty}}{V_1}\right)\Big/\left[1+\left(\frac{u_\infty}{V_1}\right)\right]}. \tag{57}$$

where u_∞/V_1 and v_∞/V_1 are evaluated by the eq. (12). Thus the turning angle change $\Delta\theta$ becomes to $\theta_f-\theta$ by the wall boundary layer effects.

In the case of the cascade test having the suction slots as shown Fig. 1, assuming the suction quantity of it is controlled to be equal to the above-mentioned value of $V_1\delta_B^*$, the turning angle θ_f' is given as follows;

$$\tan\theta_f' = \tan\theta\,\frac{1+\left(\frac{v_{f\infty}'}{V_1}\right)\Big/\left(\frac{v_\infty}{V_1}\right)}{1+\left(\frac{u_{f\infty}'}{V_1}\right)\Big/\left[1+\left(\frac{u_\infty}{V_1}\right)\right]}, \tag{58}$$

where

$$\frac{u_{f\infty}'}{V_1} = -\frac{\Delta\Gamma_q'}{V_1 H}\sin\beta_1\cos\beta_1$$

and

$$\frac{v_{f\infty}'}{V_1} = \frac{\Delta\Gamma_q'}{V_1 H}\cos^2\beta_1$$

$$\frac{\Delta\Gamma_q'}{V_1 H} = \sec^2\beta_1\int_{-\infty}^{\infty}\frac{\frac{q(\eta)}{V_1 H}}{\eta+\tan\beta_1}d\eta\,.$$

10. Numerical Examples

A few numerical examples were performed under some conditions in order to show the tendency of the wall boundary layer effects.

Assuming that the velocity distribution w is nearly equal to the uniform velocity V_1 as mentioned in the proceeding paragraph for the sake of simplicity in calculation, then the following integral in the eq. (55) becomes

$$\int_{-\infty}^{\infty}\frac{\frac{q(\eta)}{V_1 H}}{\eta+\tan\beta_1}d\eta = -\frac{1}{\pi}\int_{-\infty}^{\infty}\left(\frac{w}{V_1}\right)\left(\frac{d\delta^*}{dx}\right)\frac{d\eta}{1+\eta^2}\approx -\frac{1}{\pi}\int_{-\infty}^{\infty}\left(\frac{d\delta^*}{dx}\right)\frac{d\eta}{1+\eta^2}.$$

and, assuming that $d\delta^*/dx=d\delta_B^*/dx=$constant, which is a very crude assumption compared with the Prandtl-Kármán's theory[5]; $\delta=0.31\,(\nu/V_1x)^{\frac{1}{5}}x\propto x^{\frac{4}{5}}$, for the turbulent boundary layer along the plate, then the above integral is expressed as

$$\int_{-\infty}^{\infty}\frac{\frac{q(\eta)}{V_1H}}{\eta+\tan\beta_1}d\eta = -\frac{1}{\pi}\left(\frac{d\delta_B^*}{dx}\right)_u\int_{-\infty}^{-\tan\beta_1}\frac{d\eta}{1+\eta^2}-\frac{1}{\pi}\left(\frac{d\delta_B^*}{dx}\right)\int_{-\tan\beta_1}^{\infty}\frac{d\eta}{1+\eta^2}$$
$$= -\frac{1}{2}\left\{\left(\frac{d\delta_B^*}{dx}\right)_u+\left(\frac{d\delta_B^*}{dx}\right)_l\right\}+\frac{\beta_1}{\pi}\left\{\left(\frac{d\delta_B^*}{dx}\right)_u-\left(\frac{d\delta_B^*}{dx}\right)_l\right\},$$

where suffix u and l denotes the upper and lower wall. Using the Prandtl-Kármán's theory

$$\frac{d\delta_B^*}{dx} = 0.0173\left(\frac{\nu}{V_1H}\right)^{\frac{1}{4}}\left(\frac{\delta_B^*}{H}\right)^{-\frac{1}{4}}$$

in the above result, the induced velocities, given by the eq. (56), become

$$\frac{u_{f\infty}}{V_1} = \frac{\delta_B^*}{H}-\tan\beta_1\cdot\left(\frac{v_{f\infty}}{V_1}\right)$$
$$\frac{v_{f\infty}}{V_1} = -0.0086\,R_H^{-\frac{1}{4}}\left\{\left(\frac{\delta_B^*}{H}\right)_l^{-\frac{1}{4}}+\left(\frac{\delta_B^*}{H}\right)_u^{-\frac{1}{4}}\right\}+0.0086\beta_1\cdot R_H^{-\frac{1}{4}}\left\{\left(\frac{\delta_B^*}{H}\right)_l^{-\frac{1}{4}}-\left(\frac{\delta_B^*}{H}\right)_u^{-\frac{1}{4}}\right\}$$

where $R_H=V_1H/\nu$. Hence, the turning angle θ_f is determined by the eq. (57).

The numerical examples were performed under the following conditions; $V_1=30$ m/s, $c=75$ mm, $R_c=V_1c/\nu=1.5\times10^5$, $Z=8$, $\beta_1=\pm40°$, $\pm50°$, $\pm60°$, $C_{L_1}=1.0$ and $\delta_{B_l}^*=\delta_{B_u}^*=0.02$ m, and the results obtained are shown in Table II. These examples show one case of the thick boundary layer, but the effects of the wall boundary layer have the tendency that the change of turning angle in the retarded cascade flow is larger than the one accelarated cascade flow.

Table II

β_1	60°	50°	40°	−40°	−50°	−60°
θ_f	23° 10′	26° 0′	27° 10′	15° 30′	12° 41′	9° 45′
θ	26° 38′	29° 16′	30° 38′	16° 32′	13° 30′	10° 23′
$\Delta\theta_f$	−3° 28′	−3° 16′	−3° 28′	−1° 2′	−49′	−38′
θ_∞	23° 30′	27° 30′	29° 30′	16° 12′	13° 6′	9° 54′

Conclusion

The tunnel wall interference in cascade tests upon the turning angle and airfoil characteristics was developed by means of the conformal mapping and the Glauert's thin airfoil theory and compared with the several of the experimental results. The theoretical results of the effects on the turning angle show that the turning angles are influenced by the conditions, such as the cascade condition, numbers and arrangements of airfoils, as shown in Fig. 4, 5 and 6. The difference between the theoretical and experimental results of the airfoil characteristics, such as pressure distribution and lift coefficient, will be corrected by the boundary layer effect along the surface of airfoil itself and both side walls, the latter being especially dealt with the three-dimensional flow problem. Finally, the effects of boundary layer along the surfaces of the upper and lower tunnel walls were theoretically calculated, but they will be generally smaller than the above-mentioned effects of boundary layer along the side walls.

Acknowledgments

The author wishes to express his sincere appreciation to Messrs. Y. Matsuoka and K. Ishida for the assistance given to the author in the tedious calculations and measurements.

References

1) A. R. Howell: R & M 2095 (1942), S. M. Bogdonoff and E. E. Hess: NACA TN. No. 1271 (1947).
2) G. Kamimoto: Trans. J.S.M.E. Vol. 17, No. 58 (1947) 32. Japan Science Review Vol. 2, No. 1 (1951).
3) J. E. Erwin and J. C. Emery: NACA TR. No. 1016 (1951), H. Schlichting: J.A.S. Vol. 21 (1954).
4) B. Hudimoto, G. Kamimoto, K. Hirose: Memoirs of Faculty of Engineering, Kyoto Univ., Vol. 12, No. 3 (1950).
5) Th. v. Kármán: ZAMM Bd. 1 (1921), 233, Ergb. d. Aerodyn. Vers.-anstalt zu Göttingen III.